

# Convergence and numerics of a multi-section method for scattering by three-dimensional rough surfaces

Eric Heinemeyer <sup>1</sup>, Marko Lindner and Roland Potthast <sup>2</sup>

October 25, 2006

## Abstract

We introduce a novel *multi-section method* for the solution of integral equations on unbounded domains. The method is applied to the rough-surface scattering problem in three dimensions, in particular to a Brakhage-Werner type integral equation for acoustic scattering by an unbounded rough surface with Dirichlet boundary condition, where the fundamental solution is replaced by some appropriate half-space Green's function.

The basic idea of the multi-section method is to solve an integral equation  $A\varphi = f$  by *approximately* solving the equation  $P_\varrho AP_\tau\varphi = P_\varrho f$  for some positive constants  $\varrho, \tau$ . Here  $P_\varrho$  is a projection operator that truncates a function to a ball with radius  $\varrho > 0$ . For a very general class of operators  $A$ , for which the Brakhage Werner equation from acoustic scattering is a particular example, we will show existence of approximate solutions to the multi-section equation and that approximate solutions to the multi-section equation approximate the true solution  $\varphi_0$  of the operator equation  $A\varphi = f$ . Finally, we describe a numerical implementation of the multi-section algorithm and provide numerical examples for the case of rough surface scattering in three dimensions.

## 1 Introduction

The goal of this work is the introduction and analysis of a new numerical scheme for a class of linear operator equations

$$(1) \quad A\varphi = f$$

where  $A$  has particular decay properties.

---

<sup>1</sup>Inst. Num. Appl. Math, University of Göttingen, Lotzestr. 16-18, 37083 Göttingen, Germany

<sup>2</sup>University of Reading, Department of Mathematics, Whiteknights, PO Box 220, Berkshire, RG6 6AX, UK. Email: r.w.e.potthast@reading.ac.uk.

**Model Problem.** The basic model problem for our work is the solution of integral equations over unbounded domains which appear in what is usually called the *rough surface scattering problem* in the engineering literature. It denotes scattering of acoustic or electromagnetic waves by a surface which is a non-local perturbation of an infinite plane surface. We will restrict our attention to the case where the scattering surface

$$(2) \quad \Gamma = \{x = (x_1, x_2, x_3) \in \mathbb{R}^3 : x_3 = f(x_1, x_2)\}$$

is the graph of some bounded continuous function  $f : \mathbb{R}^2 \rightarrow \mathbb{R}$ . The domain of wave propagation is the upper perturbed half-space

$$(3) \quad D := \{x = (x_1, x_2, x_3) : x_3 > f(x_1, x_2)\}.$$

For this work we will assume that  $f \in C^{1,\alpha}$ ,  $\alpha \in (0, 1)$ , is a Lyapunov function, i.e. it is continuously differentiable with Hölder continuous first derivative.

Rough surface scattering problems arise in important applications for acoustic and electromagnetic waves. Well-known areas are outdoor sound propagation or optical scattering in nano-technology. We refer to the extensive literature reviewed in [9], [13], [12], [14] and [4]. Recently, Chandler-Wilde, Heinemeyer and Potthast [1], [2] provided some rigorous existence theory for the integral equation approach in three dimensions. But to our knowledge there is no rigorous numerical analysis for the solution of these integral equations in three dimensions. This is the starting point of our work.

However, the approach presented here is based only on very general properties of the operator equations under consideration. We expect that it can be used for a whole range of different problems, and it will be the starting point for further research.

**The Finite Section Method.** If we regard (1) as an equation on the space  $Y = L^2(\mathbb{R}^2)$ , for example, then the well-known *finite section method* consists in replacing (1) by

$$(4) \quad P_\varrho A P_\varrho \varphi = P_\varrho f,$$

where  $\varrho > 0$  and the projection operator  $P_\varrho : Y \rightarrow Y$ , is given by

$$(5) \quad (P_\varrho \psi)(x) := \begin{cases} \psi(x), & |x| < \varrho \\ 0, & \text{otherwise.} \end{cases}$$

The operator  $P_\varrho$  truncates a function on  $\mathbb{R}^2$  to its values inside the disk

$$(6) \quad B_\varrho := \{x \in \mathbb{R}^2 : |x| < \varrho\}.$$

In these notations  $|\cdot|$  denotes an arbitrary norm in  $\mathbb{R}^2$ . In particular, in our numerical part in Section 4 we will use the maximum norm  $|x| := \max(|x_1|, |x_2|)$ .

So the finite section method (4) simply restricts the right-hand side  $f$ , the solution  $\varphi$  and the resulting function  $A\varphi$  all to the same disk  $B_\varrho$ . The idea behind this method is, provided equation (1) is uniquely solvable for every right-hand side  $f$ , to hope that also equation (4) is uniquely solvable (now in  $L^2(B_\varrho)$ , of course) and that its solution  $\varphi$  approximates the exact solution  $\varphi_0$  of (1) if only one chooses  $\varrho$  large enough. If this is the case, then this method is called applicable. There are, however, simple examples of operators  $A$  that show that the finite section method is not necessarily applicable in general.

There are recent results on the applicability of the finite section method for the fairly large class of all so-called band-dominated operators in terms of their limit operators (see [7], [10] and [11]). The operators originating from 2D rough surface scattering are band-dominated, and we refer to [8], [3] and further literature cited therein for the study and application of the finite section method to these equations. Although, also for 3D rough surface scattering, the corresponding operators belong to this class, we will leave the finite section method aside and study what we call the multi-section method. We underline that the framework for this method not only covers the set of band-dominated operators, it even applies to the much larger class, called  $L(Y, \mathcal{P})$  in [7] and [10], that consists of all bounded linear operators  $A$  on  $Y$  for which

$$(7) \quad \|(I - P_\varrho)AP_\tau\| \rightarrow 0 \quad \text{and} \quad \|P_\tau A(I - P_\varrho)\| \rightarrow 0 \quad \text{as} \quad \varrho \rightarrow \infty$$

for every fixed  $\tau > 0$ . In fact, the multi-section method to be presented here only requires the first condition in (7) to be true.

**The Multi-Section Method.** Already very simple examples like the shift operator

$$(A\varphi)(x) = \varphi(x - a), \quad x \in \mathbb{R}^2$$

on  $Y = L^2(\mathbb{R}^2)$  with a fixed  $a \in \mathbb{R}^2 \setminus \{0\}$  show that the finite section method fails to apply in general. Indeed,  $P_\varrho AP_\varrho$  is neither surjective nor injective on  $L^2(B_\varrho)$ , however large  $\varrho$  is chosen. The new method proposed here will overcome some of these difficulties and will, in fact, apply to all bounded linear operators on  $Y$  that are subject to the first condition in (7).

In contrast to exactly solving the truncated equation (4); that is

$$P_\varrho AP_\varrho \varphi = P_\varrho f,$$

for large  $\varrho$ , we propose to look for a function  $\varphi \in Y$  with

$$(8) \quad P_\varrho AP_\tau \varphi \approx P_\varrho f$$

for large  $\varrho, \tau$  and a given discrepancy allowance  $\delta$  in the ' $\approx$ ' sign. So we have two main differences to the finite section method:

- (a) We allow two different cut-off parameters  $\varrho$  and  $\tau$  instead of just one.
- (b) We work with approximate instead of exact solutions.

Point (a) is the reason why we call this method the *multi-section method*. From the matrix perspective it means that we cut rectangular rather than quadratic finite matrices out of the original infinite matrix that represents our operator  $A$ .

We will show that for every precision  $\delta > 0$  and every sufficiently large parameter  $M > 0$ , there are positive constants  $\varrho, \tau$  such that there exists a function  $\varphi \in Y$  which satisfies the conditions

$$(9) \quad P_\tau \varphi = \varphi$$

$$(10) \quad \|P_\varrho AP_\tau \varphi - P_\varrho f\|_Y \leq \delta,$$

i.e.  $\varphi$  is supported on  $B_\tau$  and it approximately satisfies the multi-section equation (8).

In our main convergence result we show that, given any  $\varepsilon > 0$ , we can choose the parameters  $\delta, \varrho, \tau$  such that every solution  $\varphi$  of the multi-section method (9)–(10) approximates the true solution  $\varphi_0$  of the original equation (1) with

$$\|\varphi - \varphi_0\|_Y \leq \varepsilon.$$

**Contents of the Paper.** Section 2 introduces the three-dimensional rough surface scattering problems. Here we study the operators arising from this application and prove that they satisfy the conditions on which the multi-section method is built. Section 3 contains the main analysis for the multi-section method. We provide this analysis in a very general setting which reflects the potential of this method. Section 4 provides details about the algorithmical realization of the multi-section method and numerical examples which demonstrate the applicability of the ideas.

## 2 Scattering by rough surfaces

We restrict our attention to time-harmonic acoustic waves, which are modelled by the *Helmholtz equation*

$$(11) \quad \Delta u + \kappa^2 u = 0.$$

Here,  $\kappa$  denotes the wave number, which for the real-valued case is linked to the speed of sound  $c$  and the frequency  $\omega$  via  $\kappa = \omega/c > 0$ . Often,  $\kappa$  is admitted to be a complex number  $\kappa = \kappa_0 + i\sigma$ , where the imaginary part  $\sigma$  models the properties of some lossy medium.

For our scattering surface  $\Gamma$  we assume that  $f \in BC^{1,\alpha}(\mathbb{R}^2)$  for some  $\alpha \in (0, 1]$ . Further,  $f$  is assumed to satisfy the bounds

$$(12) \quad 0 < f^- \leq f(x) \leq f^+, \quad x \in \mathbb{R}^2.$$

We consider the scattering of an *incident acoustic wave*  $u^i$  by the surface  $\Gamma$ . The *total field*  $u := u^i + u^s$  is the sum of the incident field and the *scattered field*  $u^s$ . The scattered field is a solution to the Helmholtz equation (11) in  $D$ . Further, we assume that  $u$  satisfies the *Dirichlet boundary condition*

$$(13) \quad u(x) = 0, \quad x \in \Gamma.$$

The scattered field is required to be bounded in  $D$ , i.e.

$$(14) \quad |u^s(x)| \leq c, \quad x \in D,$$

for some constant  $c$ . Further, we follow [2] and require that  $u$  satisfies the *limiting absorption principle* as follows. If  $u$  is considered in its dependence on the complex wave number  $\kappa$ , we write  $u = u^{(\kappa)}$ . We assume that, for all sufficiently small  $\sigma > 0$ , a solution of (11), (13), (14) exists and satisfies

$$(15) \quad u^{(\kappa_0 + i\sigma)} \rightarrow u^{(\kappa_0)}, \quad \sigma \rightarrow 0$$

for all  $x \in D$ . The limiting absorption principle is a kind of radiation condition which is needed to obtain the physically correct solution to the scattering problem.

The free-space fundamental solution in three dimensions is given by the function

$$(16) \quad \Phi(x, y) = \frac{1}{4\pi} \frac{e^{i\kappa|x-y|}}{|x-y|}, \quad x \neq y \in \mathbb{R}^3.$$

The decay of this function for  $|y| \rightarrow \infty$  is very weak and it has not been possible to use it for the solution of scattering problems over unbounded domains in three dimensions. However, in [1] Chandler-Wilde, Heinemeyer and Potthast employ the Green's function for the half-space  $\{x \in \mathbb{R}^3 : x_3 > 0\}$

$$(17) \quad G(x, y) := \Phi(x, y) - \Phi(x, y')$$

with  $y' := (y_1, y_2, -y_3)$  to derive an integral equation of the second kind for the solution of the rough surface scattering problem. The decay of the function  $G$  is given in [1], equation (3.8), as

$$(18) \quad \left| G(x, y) \right| \leq \frac{C}{|x - y|^2},$$

for all  $x, y \in \mathbb{R}^3$  with  $f^- < x_3, y_3 < f^+$  with some constant  $C$ . For the normal derivative of  $G$  the estimate

$$(19) \quad \left| \frac{\partial G(x, y)}{\partial \nu(y)} \right| \leq \frac{C}{|x - y|^2},$$

holds for all  $x, y \in \mathbb{R}^3$  with  $f^- < x_3, y_3 < f^+$  with some constant  $C$ , compare equation (3.11) in [1].

We are now prepared to formulate the scattering problem under consideration.

**DEFINITION 2.1** (Point source rough surface scattering problem). *For the incident field  $u^i(x) := \Phi(x, z)$  with  $z \in D$  we seek a scattered field  $u^s \in C^2(D) \cap C(\overline{D})$  which satisfies the Helmholtz equation (11) in  $D$ , the Dirichlet boundary condition (13) on  $\Gamma$ , the bound (14) and the limiting absorption principle (15).*

The rough surface scattering problem is transformed into a boundary value problem via the Ansatz

$$(20) \quad u^s(x) = \Phi(x, z') + v(x)$$

where  $v$  satisfies the Helmholtz equation (11), the bound (14), the limiting absorption principle (15) and the boundary condition

$$(21) \quad v(x) = g(x), \quad x \in \Gamma$$

with

$$(22) \quad g(x) := -(\Phi(x, z) - \Phi(x, z')) = -G(x, z).$$

A solution to the boundary value problem can be found via the single- and double-layer potential approach. We define the *single-layer potential*

$$(23) \quad u_1(x) = \int_{\Gamma} G(x, y) \varphi(y) ds(y), \quad x \in \mathbb{R}^3,$$

and the *double-layer potential*

$$(24) \quad u_2(x) = \int_{\Gamma} \frac{\partial G(x, y)}{\partial \nu(y)} \varphi(y) ds(y), \quad x \in \mathbb{R}^3.$$

The boundary values of these potentials can be calculated using the boundary integral operators  $S$  and  $K$  defined by

$$(25) \quad (S\varphi)(x) = 2 \int_{\Gamma} G(x, y) \varphi(y) ds(y), \quad x \in \Gamma,$$

and the *double-layer potential*

$$(26) \quad (K\varphi)(x) = 2 \int_{\Gamma} \frac{\partial G(x, y)}{\partial \nu(y)} \varphi(y) ds(y), \quad x \in \Gamma.$$

It is shown in [1] that the combined single- and double layer potential

$$(27) \quad v(x) := u_2(x) - i\eta u_1(x), \quad x \in D,$$

with parameter  $\eta > 0$  satisfies the boundary value problem (21) if and only if the density  $\varphi \in L^2(\Gamma)$  satisfies the integral equation

$$(28) \quad (I + K - i\eta S)\varphi = 2g,$$

which is of the form  $(I - W)\varphi = f$  with  $W = -K + i\eta S$  and  $f = 2g$ . The basic uniqueness and existence result is given by Theorem 3.4 of [2] as follows.

**THEOREM 2.2.** *The operator  $I + K - i\eta S$  is boundedly invertible on  $L^2(\Gamma)$ , and for the norm of its inverse, one has*

$$(29) \quad \|(I + K - i\eta S)^{-1}\| \leq B,$$

where the constant  $B$ , as given in (3.4) in [2], only depends on the quotient  $\kappa/\eta$  and the Lipschitz constant of  $f$ .

As a result of Theorem 2.2 we obtain the existence of the solution for the rough surface scattering problem. In principle, the solution to the scattering problem is given by the combined potential (27) with a density  $\varphi$  which satisfies (28). Our main topic here is the numerical solution of such integral equations in three dimensions. We need to treat the numerical integration of functions over unbounded surfaces.

### 3 The multi-section method (MSM)

We will formulate our multi-section method for the following abstract setting which includes the rough surface scattering problems discussed above.

Let  $Y$  be a Banach space, and let  $\{P_\varrho\}_{\varrho>0}$  be a family of linear operators on  $Y$  with the following three properties,

- (P1)  $P_\varrho P_\tau = P_\tau = P_\tau P_\varrho$  for all  $\varrho \geq \tau > 0$ ,
- (P2)  $\|P_\varrho\| = 1$  for all  $\varrho > 0$ ,
- (P3)  $P_\varrho \rightarrow I$ , that means  $P_\varrho \varphi \rightarrow \varphi$  for all  $\varphi \in Y$ , as  $\varrho \rightarrow \infty$ .

From (P1) with  $\varrho = \tau$  we get that every  $P_\varrho$  is a projection operator. We will also have to deal with the complementary projectors  $I - P_\varrho$  which, for brevity, shall be denoted by  $Q_\varrho$ , for every  $\varrho > 0$ .

Now suppose  $A$  is a bounded linear operator on  $Y$  with

- (A1)  $A$  is invertible (and therefore boundedly invertible) on  $Y$ ,
- (A2)  $\|Q_\varrho A P_\tau\| \rightarrow 0$  as  $\varrho \rightarrow \infty$  for every fixed  $\tau > 0$ .

For illustration we give an example of  $Y$ ,  $\{P_\varrho\}_{\varrho>0}$  and  $A$  that includes the setting from equation (28) in Section 2.

**EXAMPLE 3.1.** Let  $Y = L^p(\mathbb{R}^n)$  with  $1 \leq p < \infty$  and  $n \in \mathbb{N}$ , and define  $P_\varrho$  as in (5), for every  $\varrho > 0$ . Then  $Y$  and the family  $\{P_\varrho\}_{\varrho>0}$  are clearly subject to our assumptions (P1)–(P3).

Now let  $A = I - W$ , where  $W$  is a well-defined and bounded integral operator

$$(30) \quad (W\varphi)(x) = \int_{\mathbb{R}^n} k(x, y) \varphi(y) dy, \quad x \in \mathbb{R}^n$$

on  $Y$  with the decay condition

$$(31) \quad |k(x, y)| \leq \frac{C}{|x - y|^\gamma} \quad \text{for } |x - y| > 1$$

on the kernel function  $k$ , where  $C > 0$  and  $\gamma > 0$  are some fixed constants.

Note that this example, with  $p = n = \gamma = 2$ , covers the operators in the boundary integral formulation (28) arising from 3D rough surface scattering problems as discussed in Section 2.

The following lemma shows that our assumption (A2) automatically holds for the operator  $A$  from Example 3.1 if  $\gamma p > n$ .



LEMMA 3.2. Let  $A = I - W$  act boundedly on  $Y = L^p(\mathbb{R}^n)$  with  $1 \leq p < \infty$ ,  $n \in \mathbb{N}$  and  $W$  as in (30) and (31) with  $C > 0$  and  $\gamma > 0$ . Then, for every  $\tau > 0$ , we have

$$(32) \quad \|Q_\varrho AP_\tau\| \leq \frac{c}{\varrho^{\gamma-n/p}}, \quad \varrho > 2\tau$$

with some constant  $c > 0$  depending on  $\tau$ . In particular, if  $\gamma p > n$ , then assumption (A2) holds.

*Proof.* Let  $B_\varrho = \{x \in \mathbb{R}^n : |x| \leq \varrho\}$  and  $\partial B_\varrho = \{x \in \mathbb{R}^n : |x| = \varrho\}$  be the ball and sphere of radius  $\varrho > 0$  in  $\mathbb{R}^n$ , and denote their  $n$ - and  $(n-1)$ -dimensional measure by  $|B_\varrho|$  and  $|\partial B_\varrho|$ , respectively. Now take some  $\varrho > 2\tau > 0$  and first suppose  $1 < p < \infty$ . Using Hölder's inequality with  $1/p + 1/q = 1$  we get the following.

$$\begin{aligned} \|Q_\varrho AP_\tau \varphi\|_{L^p(\mathbb{R}^n)}^p &= \int_{|x| \geq \varrho} |(AP_\tau \varphi)(x)|^p dx \\ &= \int_{|x| \geq \varrho} |(WP_\tau \varphi)(x)|^p dx \\ &= \int_{|x| \geq \varrho} \left| \int_{|y| < \tau} k(x, y) \varphi(y) dy \right|^p dx \\ &\leq \int_{|x| \geq \varrho} \left( \left( \int_{|y| < \tau} |k(x, y)|^q dy \right)^{1/q} \cdot \|P_\tau \varphi\|_{L^p(\mathbb{R}^n)} \right)^p dx \\ &\leq \int_{|x| \geq \varrho} \left( \int_{|y| < \tau} |k(x, y)|^q dy \right)^{p/q} dx \cdot \|\varphi\|_{L^p(\mathbb{R}^n)}^p \end{aligned}$$

Consequently, using the bound (31) and the inequality

$$|x| \geq \varrho > 2\tau > 2|y|, \quad \text{which implies} \quad |x - y| \geq |x| - |y| > |x|/2,$$

we get

$$\begin{aligned} \|Q_\varrho AP_\tau\|^p &\leq \int_{|x| \geq \varrho} \left( \int_{|y| < \tau} \frac{C^q}{|x - y|^{\gamma q}} dy \right)^{p/q} dx \\ &\leq \int_{|x| \geq \varrho} \left( \int_{|y| < \tau} \frac{C^q}{(|x|/2)^{\gamma q}} dy \right)^{p/q} dx \\ &= \left( \int_{|x| \geq \varrho} \frac{1}{|x|^{\gamma p}} dx \right) \left( \int_{|y| < \tau} dy \right)^{p/q} 2^{\gamma p} C^p \end{aligned}$$

$$\begin{aligned}
&= \left( \int_{r=\varrho}^{+\infty} \frac{1}{r^{\gamma p}} |\partial B_r| dr \right) |B_\tau|^{p/q} 2^{\gamma p} C^p \\
&= \left( \int_{r=\varrho}^{+\infty} \frac{r^{n-1}}{r^{\gamma p}} dr \right) |\partial B_1| |B_\tau|^{p/q} 2^{\gamma p} C^p \\
(33) \quad &= \varrho^{n-\gamma p} \frac{1}{\gamma p - n} |\partial B_1| |B_\tau|^{p/q} 2^{\gamma p} C^p.
\end{aligned}$$

Finally, taking  $p$ -th roots proves (32). The proof for  $p = 1$  is similar. But instead of using Hölder's inequality one immediately arrives at (33), with  $p/q$  replaced by 0.  $\square$

We illustrate the generality of our approach with three more examples of Banach spaces  $Y$  with projections  $P_\varrho$  and operators  $A$  acting on them.

**EXAMPLE 3.3.** Let  $Y = \ell^p(\mathbb{Z}^n)$  with  $1 \leq p < \infty$  and  $n \in \mathbb{N}$ . Define  $P_\varrho$ , with  $\varrho > 0$ , literally as in (5) but with  $x \in \mathbb{Z}^n$ , of course. Also here, (P1)–(P3) clearly hold.

In this case, in fact every bounded linear operator  $A$  on  $Y$  is subject to (A2)! This can be seen as follows. Since all  $P_\tau$  are compact operators on  $Y$ , also  $AP_\tau$  is compact for every  $\tau > 0$ . But since, by (P3),  $Q_\varrho \rightarrow 0$  as  $\varrho \rightarrow \infty$ , and since point-wise convergence on compact sets is uniformly, we get that even (A2) holds.

**EXAMPLE 3.4.** Let  $Y = C[0, 1]$ . For  $m \in \mathbb{N}$ , let  $P_m\varphi$  denote the piece-wise linear function which interpolates  $\varphi \in Y$  at the points  $j/2^m$  with  $j = 0, \dots, 2^m$ , and for arbitrary  $\varrho > 0$ , put  $P_\varrho = P_{[\varrho]}$  with  $[\varrho]$  denoting the integer part of  $\varrho$ . Then it is easy to see that (P1)–(P3) are fulfilled.

**EXAMPLE 3.5.** Let  $Y = L^2(\mathbb{T})$  where  $\mathbb{T} := \{z \in \mathbb{C} : |z| = 1\}$  is the complex unit circle. For  $m \in \mathbb{N}$ , let

$$(P_m\varphi)(t) = \sum_{k=-m}^m c_k t^k, \quad t \in \mathbb{T}$$

be the truncated Fourier series of  $\varphi$  with  $c_k$  denoting its  $k$ -th Fourier coefficient. And again put  $P_\varrho = P_{[\varrho]}$  for arbitrary  $\varrho > 0$ . Then (P1)–(P3) are fulfilled.

Note that this example is isometrically isomorphic to Example 3.3 with  $n = 1$  and  $p = 2$ , the isomorphism being the Fourier transform. As a result we get that also here every bounded linear operator  $A$  on  $Y$  is subject to (A2).

Given a Banach space  $Y$  and a family of projections  $\{P_\varrho\}_{\varrho>0}$  on  $Y$  with properties (P1)–(P3), an operator  $A$  on  $Y$  with properties (A1) and (A2), and an arbitrary

element  $f \in Y$ , we are looking for the (unique) solution  $\varphi =: \varphi_0$  of (1); that is

$$A\varphi = f.$$

For the approximate solution of equation (1) we propose the following method.

**DEFINITION 3.6** (Multi-section method (MSM)). *For given precision  $\delta > 0$  and sufficiently large cut-off parameters  $\varrho$  and  $\tau$ , calculate a solution  $\varphi \in Y$  of the system*

$$\left. \begin{array}{l} P_\tau \varphi = \varphi \\ \|P_\varrho A P_\tau \varphi - P_\varrho f\| \leq \delta. \end{array} \right\} \quad (\text{MSM})$$

**THEOREM 3.7** (Existence of solutions to (MSM)). *For every  $\delta > 0$ , there is a  $\tau_0 = \tau_0(\delta) > 0$  such that, for all parameters  $\varrho > 0$  and  $\tau > \tau_0$ , the system (MSM) is solvable in  $Y$ .*

**DEFINITION 3.8.** *We say that  $\tau_0 > 0$  is an admissible  $\tau$ -bound for a given precision  $\delta > 0$  if (MSM) is solvable in  $Y$  for all  $\varrho > 0$  and  $\tau > \tau_0$ .*

*Proof of Theorem 3.7.* Let  $\varrho > 0$  be arbitrary. We demonstrate how to choose  $\tau_0$  so that

$$(34) \quad \varphi_1 := P_\tau \varphi_0 = P_\tau A^{-1} f$$

solves the system (MSM) for every  $\tau > \tau_0$ , with  $\varphi_0$  being the exact solution of (1).

Since  $P_\tau$  is a projector, we have

$$P_\tau \varphi_1 = P_\tau^2 \varphi_0 = P_\tau \varphi_0 = \varphi_1$$

for every  $\tau > 0$ .

Furthermore, for all  $\varrho > 0$  and  $\tau > 0$ , we have

$$\begin{aligned} \|P_\varrho A P_\tau \varphi_1 - P_\varrho f\| &= \|P_\varrho A P_\tau^2 A^{-1} f - P_\varrho f\| \\ &\leq \|P_\varrho A A^{-1} f - P_\varrho f\| + \|P_\varrho A Q_\tau A^{-1} f\| \\ &\leq 0 + \|A\| \cdot \|Q_\tau A^{-1} f\|. \end{aligned}$$

But, by assumption (P3), there is a  $\tau_0 > 0$  such that

$$(35) \quad \|Q_\tau A^{-1} f\| \leq \frac{\delta}{\|A\|}$$

for all  $\tau > \tau_0$ , so that finally

$$\|P_\varrho A P_\tau \varphi_1 - P_\varrho f\| \leq \delta$$

holds, and hence  $\varphi_1$  is a solution of the system (MSM) for all  $\tau > \tau_0$  and  $\varrho > 0$ .  $\square$

LEMMA 3.9. *Let  $\tau_0 > 0$  be an admissible  $\tau$ -bound for a given precision  $\delta > 0$ . If  $\tau > \tau_0$  and  $\varrho > 0$  are such that  $\|Q_\varrho AP_\tau\| < 1/\|A^{-1}\|$ , then the set of all solutions of (MSM) is a bounded subset of  $Y$ . Precisely, every solution  $\varphi \in Y$  of the system (MSM) is subject to  $\|\varphi\|_Y \leq M$  with  $M$  given by (36).*

*Proof.* Suppose  $\varphi \in Y$  solves (MSM) for given parameters  $\delta, \varrho, \tau > 0$ . Then

$$\begin{aligned} \|A\varphi\| - \|P_\varrho f\| &\leq \|A\varphi - P_\varrho f\| = \|AP_\tau\varphi - P_\varrho f\| \\ &\leq \|AP_\tau\varphi - P_\varrho AP_\tau\varphi\| + \|P_\varrho AP_\tau\varphi - P_\varrho f\| \\ &\leq \|Q_\varrho AP_\tau\| \cdot \|\varphi\| + \delta \end{aligned}$$

together with  $\|\varphi\| \leq \|A^{-1}\| \cdot \|A\varphi\|$  implies that

$$\begin{aligned} \frac{\|\varphi\|}{\|A^{-1}\|} &\leq \|A\varphi\| \leq \|P_\varrho f\| + \|Q_\varrho AP_\tau\| \cdot \|\varphi\| + \delta \\ &\leq \|f\| + \|Q_\varrho AP_\tau\| \cdot \|\varphi\| + \delta \end{aligned}$$

and hence

$$(36) \quad \|\varphi\| \leq M := \frac{\|f\| + \delta}{1/\|A^{-1}\| - \|Q_\varrho AP_\tau\|}.$$

□

THEOREM 3.10 (Convergence of the MSM). *For every  $\varepsilon > 0$ , there are parameters  $\delta, \varrho, \tau$  such that every solution  $\varphi \in Y$  of the system (MSM) is an approximation*

$$(37) \quad \|\varphi - \varphi_0\|_Y < \varepsilon$$

*of the exact solution  $\varphi_0$  of (1). Precisely, there are functions  $\delta_0, \tau_0 : \mathbb{R}_+ \rightarrow \mathbb{R}_+$  and  $\varrho_0 : \mathbb{R}_+^3 \rightarrow \mathbb{R}_+$  such that if  $\delta < \delta_0(\varepsilon)$ ,  $\tau > \tau_0(\delta)$  and  $\varrho > \varrho_0(\varepsilon, \delta, \tau)$ , then every solution  $\varphi \in Y$  of (MSM) is subject to (37).*

*Proof.* Let  $\varepsilon > 0$  be given.

(a) Choose  $\delta < \delta_0 := \frac{\varepsilon}{3\|A^{-1}\|}$ .

(b) Choose  $\tau_0 > 0$  such that  $(\|Q_\tau\varphi_0\| = )\|Q_\tau A^{-1}f\| \leq \frac{\delta}{\|A\|}$  for all  $\tau > \tau_0$ , so that  $\tau_0$  is an admissible  $\tau$ -bound for  $\delta$  (see inequality (35)). Now let  $\tau > \tau_0$ .

(c) Choose  $\varrho_0 > 0$  such that  $\|Q_\varrho f\| < \frac{\varepsilon}{3\|A^{-1}\|}$  and

$$(38) \quad \|Q_\varrho AP_\tau\| < \frac{1}{\|A^{-1}\|} \left( 1 - \frac{1}{1 + \frac{\varepsilon}{3(\|f\| + \delta) \cdot \|A^{-1}\|}} \right)$$

for all  $\varrho > \varrho_0$ , and fix some  $\varrho > \varrho_0$ .

Now let  $\varphi \in Y$  be a solution of (MSM) with parameters  $\delta, \tau$  and  $\varrho$  as chosen above. From (38) we get  $\|Q_\varrho AP_\tau\| < 1/\|A^{-1}\|$ , and hence, by Lemma 3.9,

$$(39) \quad \|\varphi\| \leq M$$

with  $M$  as defined in (36). Moreover, inequality (38) is equivalent to

$$\|Q_\varrho AP_\tau\| < \frac{1}{\|A^{-1}\|} \cdot \frac{\frac{\varepsilon}{3(\|f\|+\delta) \cdot \|A^{-1}\|}}{1 + \frac{\varepsilon}{3(\|f\|+\delta) \cdot \|A^{-1}\|}},$$

and hence to

$$\left(1 + \frac{\varepsilon}{3(\|f\| + \delta) \cdot \|A^{-1}\|}\right) \cdot \|Q_\varrho AP_\tau\| < \frac{1}{\|A^{-1}\|} \cdot \frac{\varepsilon}{3(\|f\| + \delta) \cdot \|A^{-1}\|}.$$

This, moreover, is equivalent to

$$(40) \quad \begin{aligned} \|Q_\varrho AP_\tau\| &< \frac{1}{\|A^{-1}\|} \cdot \frac{\varepsilon}{3(\|f\| + \delta) \cdot \|A^{-1}\|} - \frac{\varepsilon}{3(\|f\| + \delta) \cdot \|A^{-1}\|} \cdot \|Q_\varrho AP_\tau\| \\ &= \frac{\varepsilon(1/\|A^{-1}\| - \|Q_\varrho AP_\tau\|)}{3(\|f\| + \delta) \cdot \|A^{-1}\|} = \frac{\varepsilon}{3M\|A^{-1}\|} \end{aligned}$$

with  $M$  as defined in (36). Then we have

$$\begin{aligned} \|\varphi - \varphi_0\| &= \|P_\tau \varphi - \varphi_0\| = \|A^{-1}AP_\tau \varphi - A^{-1}f\| \leq \|A^{-1}\| \cdot \|AP_\tau \varphi - f\| \\ &\leq \|A^{-1}\| \cdot (\|AP_\tau \varphi - P_\varrho AP_\tau \varphi\| + \|P_\varrho AP_\tau \varphi - P_\varrho f\| + \|P_\varrho f - f\|) \\ &\leq \|A^{-1}\| \cdot (\|Q_\varrho AP_\tau\| \cdot \|\varphi\| + \delta + \|Q_\varrho f\|) \\ &\leq \frac{\varepsilon}{3} + \frac{\varepsilon}{3} + \frac{\varepsilon}{3} = \varepsilon, \end{aligned}$$

using inequalities (40) and (39) and the bounds on  $\delta$  and  $\|Q_\varrho f\|$  in the last step.  $\square$

**REMARK 3.11.** *One way to effectively solve the system (MSM) for given parameters  $\varrho, \tau$  and  $\delta$  is to compute a  $\varphi \in Y$  that minimizes the discrepancy in (8), for example using a gradient method or, if possible, by directly applying the Moore Penrose pseudo-inverse  $B^\dagger$  of  $B := P_\varrho AP_\tau$  to the right-hand side  $P_\varrho f$ .*

*If  $Y$  is a Hilbert space, then it is well-known that  $\varphi \in Y$  minimizes the residual  $\|B\varphi - P_\varrho f\|$  if and only if  $B^*(B\varphi - P_\varrho f) = 0$  with  $B^*$  denoting the adjoint operator of  $B$ . If, in addition,  $P_\varrho$  is self-adjoint for all  $\varrho > 0$ , then, after re-substituting  $B$ , the latter is equivalent to*

$$(41) \quad P_\tau A^* P_\varrho AP_\tau \varphi = P_\tau A^* P_\varrho f.$$

However, if  $\varrho$  is sufficiently large, then, by (A2) and (P3), the equation (41) is just a small perturbation of

$$(42) \quad P_\tau A^* A P_\tau \varphi = P_\tau A^* f,$$

which is nothing but the finite section method for the equation

$$(43) \quad A^* A \varphi = A^* f.$$

Note that the finite section method (42) is applicable since  $A^* A$  is positive definite (see, e.g. Theorem 1.10 b in [5]). Clearly, if  $A$  is invertible, as we require in (A1), then also its adjoint  $A^*$  is invertible, and (43) is equivalent to our original equation (1).

Summarizing, if  $Y$  is a Hilbert space and all  $P_\varrho$  are self-adjoint, then minimizing  $\|P_\varrho A P_\tau \varphi - P_\varrho f\|$  is equivalent to solving a slight perturbation (41) of the finite section method (42) for (43).

The multi-section method can be applied to the rough surface scattering problem of Section 2, as we know from Example 3.1, Lemma 3.2 and inequalities (18) and (19). In particular, note that the bound (29) on  $\|A^{-1}\|$  enables us to actually compute the corresponding terms in step (a) and (c) in the proof of Theorem 3.10.

We summarize the results in the following theorem.

**THEOREM 3.12** (MSM for rough surface scattering). *The multi-section method as defined in Definition 3.6, applied to rough surface scattering (11), (13), (14) and (15), is convergent in the sense of Theorem 3.10.*

## 4 Numerical realization and examples

The goal of this final section is to provide a numerical algorithm for the solution of the integral equation (28) using the multi-section method. For simplicity, we employ a low-order scheme for the treatment of the singularity of the operator, leaving more sophisticated high-order approaches to [6].

Our numerical approach to the solution of the system (MSM) for the concrete operator equation (28) is to choose some large parameters  $\varrho$  and  $\tau$  and to choose the discrepancy  $\delta$  as small as it possibly can be by looking for a function  $\varphi \in L^2(B_\tau)$  that minimizes the MSM-residual  $\|P_\varrho A P_\tau \varphi - P_\varrho f\|$ .

We have implemented both a *direct solver* for the minimization of the corresponding MSM-residual and an *iterative scheme* based on a gradient method. In

both cases we first transform the truncated approximate equation (8) into a matrix equation which, for simplicity, we denote by

$$(44) \quad \mathbf{A}\boldsymbol{\varphi} = \mathbf{b}.$$

The direct solver then approximately solves this equation via the Moore-Penrose pseudo inverse  $\mathbf{A}^\dagger$  of  $\mathbf{A}$ . Precisely,

$$(45) \quad \boldsymbol{\varphi} = \mathbf{A}^\dagger \circ \mathbf{b}$$

has the smallest norm among all  $\boldsymbol{\varphi}$  that minimize the residual  $\|\mathbf{A}\boldsymbol{\varphi} - \mathbf{b}\|$ .

This scheme is rather quick, but limits the number of unknowns  $N$  to several thousands, since we need to store fully occupied matrices of size  $N^2$ . This leads to a bound of approximately 10 on the number of wavelengths which can be resolved, since, for example,  $N = 2500$  unknowns correspond to a grid-size of  $50 \times 50$  grid points on our surface, and we need at least 5 points per wavelength for its resolution.

For problems with more unknowns we used an iterative solver, where the functional

$$(46) \quad \mu(\boldsymbol{\varphi}) := \|\mathbf{A}\boldsymbol{\varphi} - \mathbf{b}\|^2$$

is minimized. For the minimization we employed the *gradient method*

$$(47) \quad \boldsymbol{\varphi}_{n+1} = \boldsymbol{\varphi}_n - h_n \operatorname{grad}_{\boldsymbol{\varphi}} \mu(\boldsymbol{\varphi}_n), \quad n = 0, 1, 2, \dots$$

with starting value  $\boldsymbol{\varphi} = 0$  and adaptive stepsize  $h_n > 0$ . Simple calculations show that the gradient of  $\mu$  with respect to the complex density  $\boldsymbol{\varphi}$  is given by

$$(48) \quad \operatorname{grad}_{\boldsymbol{\varphi}} \mu(\boldsymbol{\varphi}) = 2\mathbf{A}^* \circ (\mathbf{A}\boldsymbol{\varphi} - \mathbf{b}).$$

To see this one simply writes  $\boldsymbol{\varphi} \in \mathbb{C}^N$  as a function  $\tilde{\boldsymbol{\varphi}} \in \mathbb{R}^{2N}$ , calculates the gradient in  $\mathbb{R}^{2N}$  and converts it back into  $\mathbb{C}^N$ . The calculation of

$$(49) \quad \mathbf{s}_1 := \mathbf{A}\boldsymbol{\varphi},$$

$$(50) \quad \mathbf{s}_2 = \mathbf{s}_1 - \mathbf{b}$$

$$(51) \quad \operatorname{grad}_{\boldsymbol{\varphi}} \mu(\boldsymbol{\varphi}) = 2\mathbf{A}^* \circ \mathbf{s}_2$$

can be carried out without storing the matrices  $\mathbf{A}$  and  $\mathbf{A}^*$ , i.e. for the gradient method we only need to store vectors of length  $N$ . Here, in principle, we can work with up to several Million unknowns  $N$  if we can invest the time to calculate the updates. In this case we can resolve up to 400 wavelengths with a grid-size of  $2000 \times 2000$ .

For the iteration scheme the computation time per iteration scales quadratically in the number of unknowns. If we want to keep the time for one gradient step in the time-frame of hours, this limits the size of the problem to approximately  $N = 100.000$ , which corresponds to a grid of  $350 \times 350$  or a resolution of 70 wavelengths. It is clear that at this point matrix compression schemes like the fast multipole method need to be employed. Since our main point here is the presentation of the multi-section method and the proof of its applicability we leave this to future research.

The main ingredient of equation (28) is the integral operator  $I + K - i\eta S$ , which, for the MSM, is applied to some density  $P_\tau \varphi$  supported on  $B_\tau$  and is evaluated on the set  $B_\rho$ . We denote the kernel of  $K - i\eta S$  by  $k(x, y)$ ,  $x \in B_\rho$ ,  $y \in B_\tau$ .

We employ the basic ideas of Nyström's method, however applied to the approximate equation (8). We use standard numerical quadrature for the calculation of

$$(52) \quad I(x) := \int_{B_\tau} k(x, y) \varphi(y) dy, \quad x \in B_\rho,$$

i.e. we replace the integral by a finite sum

$$(53) \quad I_N(x) := \sum_{\xi=1}^N \alpha_\xi \tilde{k}(x, y_\xi) \varphi(y_\xi), \quad x \in B_\rho$$

with *quadrature points*  $y_\xi \in B_\rho$  and *weights*  $\alpha_\xi$ , where we define

$$(54) \quad \tilde{k}(x, y) = \begin{cases} k(x, y), & |x - y| \geq \tilde{\rho} \\ c(x), & |x - y| < \tilde{\rho} \end{cases}$$

with a constant  $\tilde{\rho} > 0$  and appropriately chosen values  $c(x)$ ,  $x \in \Gamma \cap B_\rho$ . For a convergent quadrature formula the values (53) approximate the integral (52) and we have

$$(55) \quad I_N(x) \rightarrow I(x), \quad N \rightarrow \infty, \quad x \in B_\rho.$$

Next, we choose points  $x_\eta \in B_\rho$  for  $\eta = 1, \dots, M$ , define

$$(56) \quad V := \{x_\eta : \eta = 1, \dots, M\}, \quad L := \{y_\xi : \xi = 1, \dots, N\}.$$

For our numerics of the direct method we chose the points such that  $L \subset V$ . Then we evaluate  $I_N(x_\eta)$  at the points  $x_\eta$ ,  $\eta = 1, \dots, M$ . This leads to the discrete system

$$(57) \quad \|\mathbf{A}\varphi - \mathbf{f}\|_2 \leq \delta$$



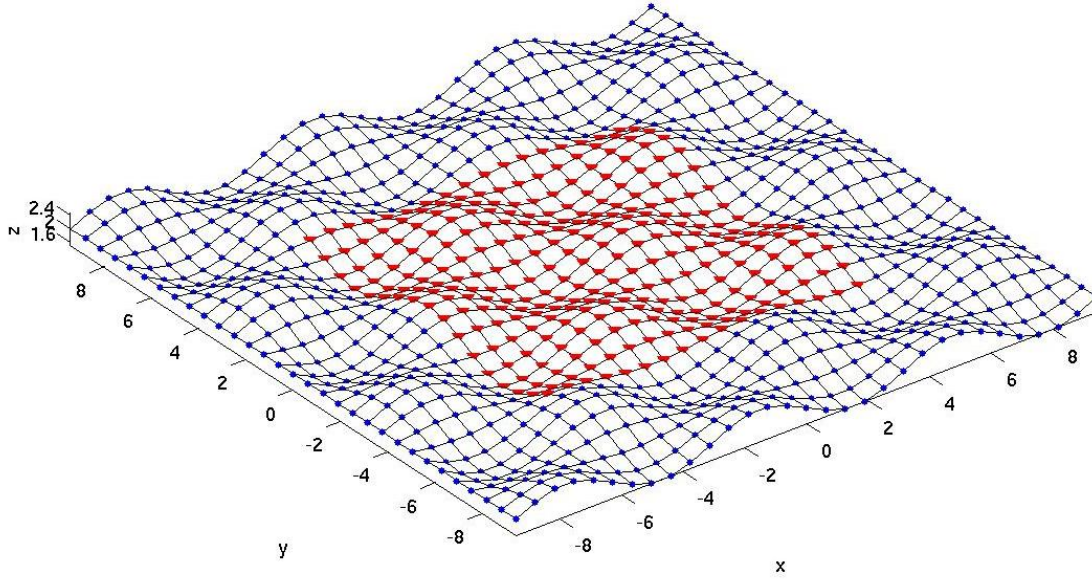


Figure 1: Setting for the multi-section method. The set  $B_\varrho$  is shown with blue dots, the set  $B_\tau$  with red triangles.

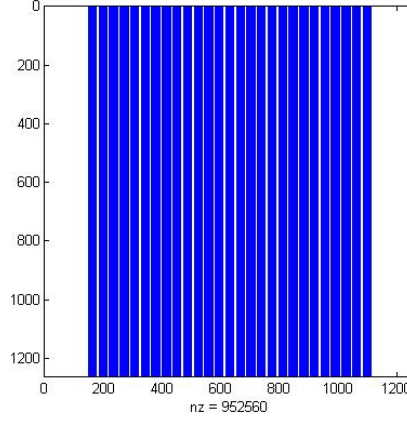
with

$$(58) \quad \mathbf{A} = (\mathbf{I} - \mathbf{W}) \circ \mathbf{P}_\tau,$$

$$(59) \quad \boldsymbol{\varphi} = \begin{pmatrix} \varphi(x_1) \\ \vdots \\ \varphi(x_M) \end{pmatrix},$$

$$(60) \quad \mathbf{f} = \begin{pmatrix} f(x_1) \\ \vdots \\ f(x_M) \end{pmatrix},$$

$$(61) \quad \mathbf{W} = \begin{pmatrix} \alpha_1 k(x_1, x_1) & \dots & \alpha_M k(x_1, x_M) \\ \vdots & & \vdots \\ \alpha_1 k(x_M, x_1) & \dots & \alpha_M k(x_M, x_M) \end{pmatrix},$$

Figure 2: Structure of the matrix  $\mathbf{A} = (\mathbf{I} - \mathbf{W}) \circ \mathbf{P}_\tau$ .

and the projector  $\mathbf{P}_\tau$  is defined by

$$(62) \quad \mathbf{P}_\tau = \text{diag}(\mathbf{v}), \quad \mathbf{v}_j = \begin{cases} 1, & \text{if } x_j \in B_\tau \\ 0, & \text{otherwise,} \end{cases}$$

for  $j = 1, \dots, M$ .

The solution of (57) is calculated using the Moore-Penrose pseudo inverse  $\mathbf{A}^\dagger$  (in Matlab realized via the function `pinv(A)`) applied to  $\mathbf{f}$ , i.e. via

$$(63) \quad \varphi_{\text{sol}} := \left( (\mathbf{I} - \mathbf{W}) \circ \mathbf{P}_\tau \right)^\dagger \mathbf{f}.$$

As a test example for the numerical realization of the multisection method we use the surface  $\Gamma$  defined by

$$f(x_1, x_2) := c_0 \cdot \sin(x_1) \cdot \cos(x_2) + 2$$

with  $c_0 = 1/2$ . Here, we place the source point  $z$  of the incident point-source  $\Phi(\cdot, z)$  below the surface  $\Gamma$ , but above the plane  $x_3 = 0$ . In this case the scattered field is given by  $-\Phi(\cdot, z)$ . Thus, we can test the precision of the combined single- and double-layer potential with density  $\varphi$  calculated via the multi-section method.

Figure 3 (a) shows the original fields for an incident point source with source point  $(-2, 0, 0.2)$ . The reconstructed field is shown in Figure 3 (b). Here, we worked with the direct method and employed the multi-section method with  $\varrho = 3\pi$  and  $\tau = 0.8 \varrho$ . The figures show a grid of  $40 \times 40$  points.

Figure 4 demonstrates the real part of the scattered field for an incident point source with source point  $(-2, 0, 4)$ . We employed the direct method and used the same choice of parameters as in Figure 3.

The behaviour of the solution density  $\varphi$  of the multi-section method is shown in Figure 5. The different sections are indicated in the third row. The right-hand side shows the 'true' density, which is calculated using larger patches.

The behaviour of the solutions for the *iterative* scheme is demonstrated in Figures 6 and 4. Figure 6 (a) is a schematic presentation of the relation between the area  $\varrho^2$  of the calculation domain, the total number of unknowns  $N$  and the one-dimensional step size  $h$ . The blue lines are lines of constant step size, where both  $N$  and  $\varrho$  are increased. To achieve convergence of the numerical method, we need to increase both  $\varrho$  and  $N$  such that  $h = h(\varrho, N)$  tends to zero.

The relative error for the calculation of the field of Figure 3 for different choices of  $\varrho$  and  $N$  is demonstrated in Figure 6 (b). For a fixed small number of unknowns the error for a large calculation domain is larger than for a small calculation domain. This can be explained by the two types of error which add up to the total error:

1. the discretization error from approximating the integral by a quadrature formula
2. the cut-off error from the limited domain of calculation.

If for a fixed number of unknowns we enlarge the calculation domain, then the cut-off error decreases, but the discretization error increases. Here with  $N = 3500$  unknowns and a sufficiently large calculation area we reach an error of 2%.

The behaviour of the residual for the gradient method is illustrated in Figure 4 (b). The error usually quickly drops and then tends to some fixed residual which does not change significantly when further iterating. The residual is caused by the discretization and cut-off error. We usually used 15-20 iterations in our calculations.

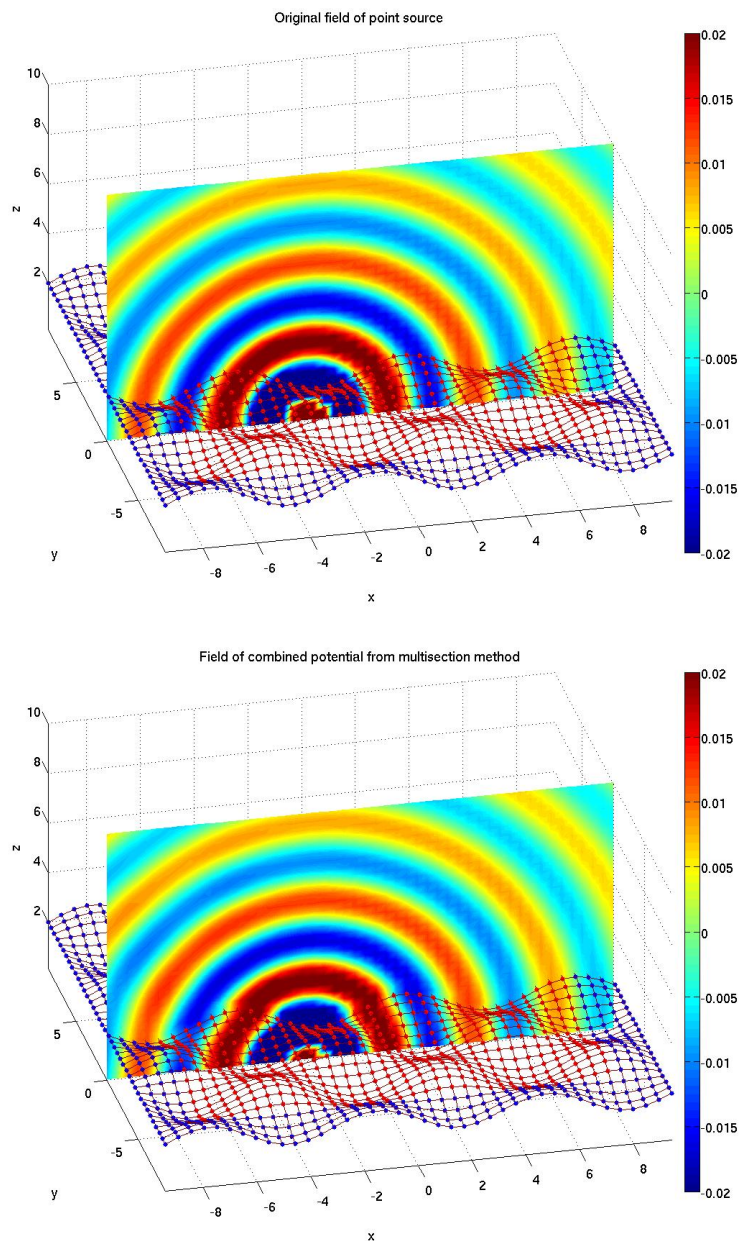


Figure 3: (a) Test field of a point source located between the surface and the plane  $x_3 = 0$ . (b) Constructed field via the combined layer potential with a density given by the multi-section method. Here, the relative error for the reconstruction in the points with  $x_3 \geq 3$  above the set  $B_\varrho$  is below 5%.

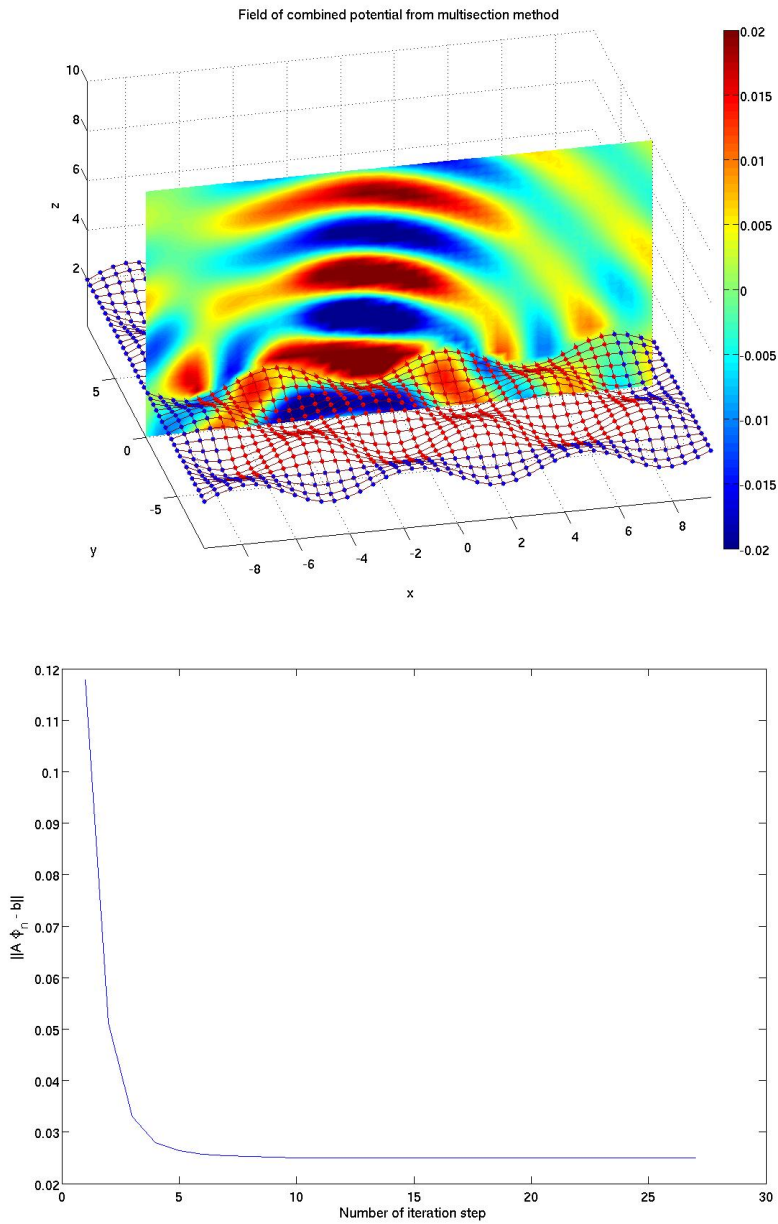


Figure 4: (a) Scattered field for an incident point source with source point  $z = (-2, 0, 4)$ . (b) Error behaviour for the iterates of the gradient method.

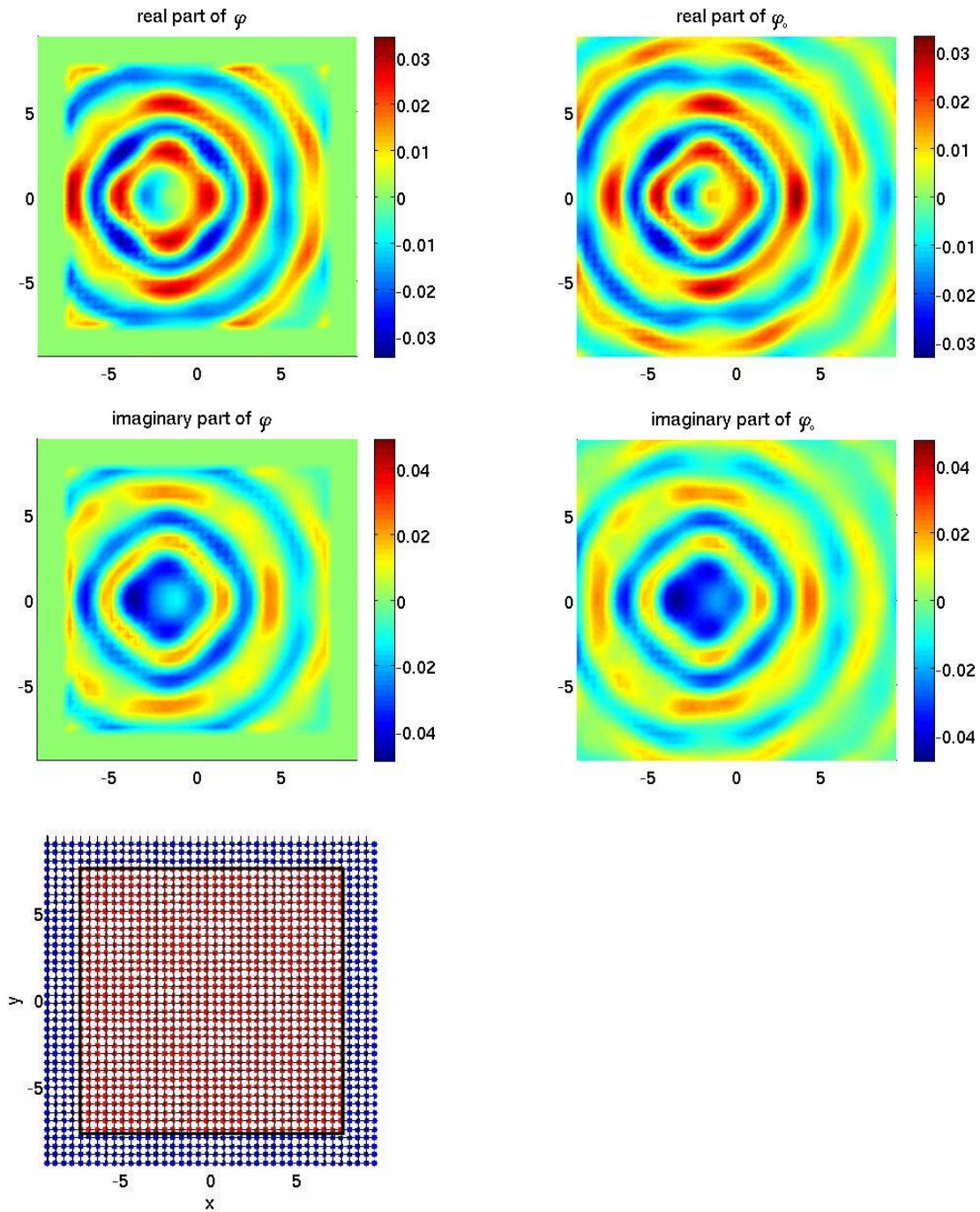


Figure 5: The images show the real and imaginary part of the density  $\varphi$  solving the multi-section inequality in the left column and the true density  $\varphi_0$  in the right column. The location of the two different sections  $B_\tau$  and  $B_\rho$  is indicated in the image of the third row. On the set  $B_\tau$  the approximation is good and on  $B_\rho \setminus B_\tau$  the density  $\varphi$  is zero by construction.

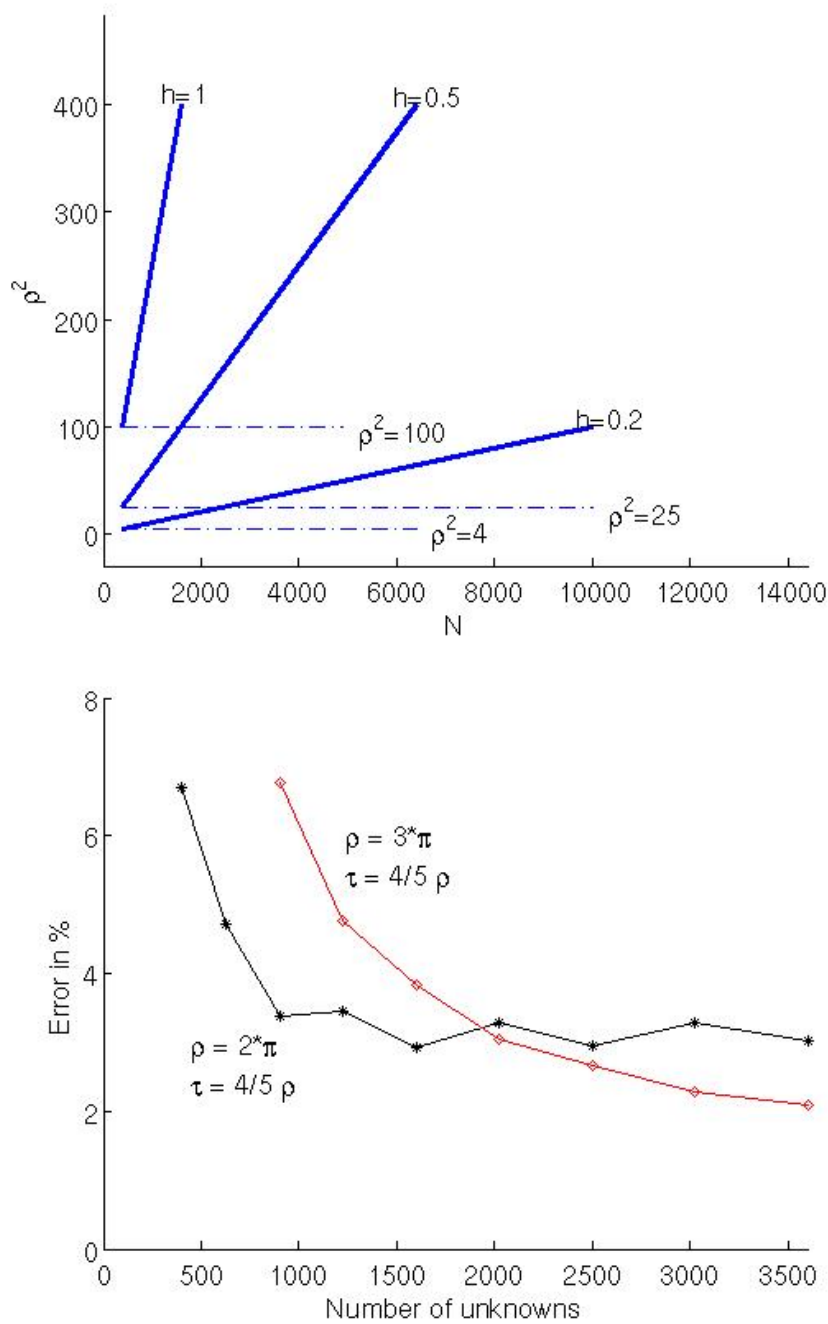


Figure 6: (a) Scheme to discuss the discretization and cut-off error and convergence properties of the multi-section method. (b) Illustration of the relative error measured in the calculated field for different choices of cut-off parameters  $\rho$  and  $\tau$  in dependence of the number of unknowns  $N$ . In both cases we have chosen a fixed ratio of  $\rho/\tau = 4/5$ . The black curve with stars shows the error for  $\rho = 2\pi$  and the red curve with diamonds shows the error for  $\rho = 3\pi$ .

## References

- [1] S. N. Chandler-Wilde, E. Heinemeyer, and R. Potthast. Acoustic scattering by mildly rough unbounded surfaces in three dimensions. *SIAM J. Appl. Math.*, 66:1002–1026, 2006.
- [2] S. N. Chandler-Wilde, E. Heinemeyer, and R. Potthast. A well-posed integral equation formulation for three-dimensional rough surface scattering. *Proceedings of the Royal Society of London, Series A*:DOI: 10.1098/rspa.2006.1752, 2006.
- [3] S. N. Chandler-Wilde and M. Lindner. Boundary integral equations on unbounded rough surfaces: Fredholmness and the finite section method. Submitted.
- [4] DeSanto. Scattering by rough surfaces. In *Scattering: Scattering and Inverse Scattering in Pure and Applied Science*, eds. R. Pike & P. Sabatier, pages 15–36. New York: Academic Press, 2002.
- [5] R. Hagen, S. Roch, and B. Silbermann. *C\*-Algebras and Numerical Analysis*. Marcel Dekker, 2001.
- [6] E. Heinemeyer. *Integral equation methods for rough surface scattering problems in three dimensions*. PhD Dissertation, Göttingen, to appear in 2007.
- [7] M. Lindner. *Infinite Matrices and their Finite Sections: An Introduction to the Limit Operator Method*. Frontiers in Mathematics. Birkhäuser Verlag, Basel, Boston, Berlin, 2006.
- [8] A. Meier and S. N. Chandler-Wilde. On the stability and convergence of the finite section method for integral equation formulations of rough surface scattering. *Math. Methods Appl. Sci.*, 24:209–232, 2001.
- [9] J. A. Ogilvy. *Theory of Wave Scattering from Random Rough Surfaces*. Bristol: Adam Hilger, 1991.
- [10] V.S. Rabinovich, S. Roch, and B. Silbermann. *Limit Operators and Their Applications in Operator Theory*, volume 150 of *Operator Theory: Advances and Applications*. Birkhäuser Verlag, Basel, Boston, Berlin, 2004.
- [11] S. Roch. Finite sections of band-dominated operators. *Technical University Darmstadt, Preprint 2355*, 2004. To appear in *Memoirs AMS*, 2006.



- [12] M. Saillard and A. Sentenac. Rigorous solutions for electromagnetic scattering from rough surfaces. *Waves Random Media*, 11:R103–R137, 2001.
- [13] A. G. Voronovich. *Wave Scattering from Rough Surfaces*. Springer, 1998 2nd Edt.
- [14] K. F. Warnick and W. C. Chew. Numerical simulation methods for rough surface scattering. *Waves Random Media*, 11:R1–R30, 2001.